

Amplification of 12 OAM Modes in an air-core erbium doped fiber

Qiongyue Kang,^{1,*} Patrick Gregg,² Yongmin Jung,¹ Ee Leong Lim,¹ Shaif-ul Alam,¹ Siddharth Ramachandran,² and David J. Richardson¹

¹Optoelectronics Research Centre, University of Southampton, Southampton, SO17 1BJ, UK

²Electrical and Computer Engineering Department, Boston University, 8 St Mary's St, Boston, MA, USA

*qk1g11@orc.soton.ac.uk

Abstract: We theoretically propose an air-core erbium doped fiber amplifier capable of providing relatively uniform gain for 12 orbital angular momentum (OAM) modes ($|L| = 5, 6$ and 7 , where $|L|$ is the OAM mode order) over the C-band. Amplifier performance under core pumping conditions for a uniformly doped core for each of the supported pump modes (110 in total) was separately assessed. The differential modal gain (DMG) was found to vary significantly depending on the pump mode used, and the minimum DMG was found to be 0.25 dB at 1550 nm provided by the OAM (8,1) pump mode. A tailored confined doping profile can help to reduce the pump mode dependency for core pumped operation and help to increase the number of pump modes that can support a DMG below 1 dB. For the more practical case of cladding-pumped operation, where the pump mode dependency is almost removed, a DMG of 0.25 dB and a small signal gain of >20 dB can be achieved for the 12 OAM modes across the full C-band.

©2015 Optical Society of America

OCIS codes: (060.2320) Fiber optics amplifiers and oscillators; (050.4865) Optical vortices; (060.4230) Multiplexing.

References and links

1. N. Bozinovic, Y. Yue, Y. Ren, M. Tur, P. Kristensen, H. Huang, A. E. Willner, and S. Ramachandran, "Terabit-scale orbital angular momentum mode division multiplexing in fibers," *Science* **340**(6140), 1545–1548 (2013).
2. J. Wang, J.-Y. Yang, I. M. Fazal, N. Ahmed, Y. Yan, H. Huang, Y. Ren, Y. Yue, S. Dolinar, M. Tur, and A. E. Willner, "Terabit free-space data transmission employing orbital angular momentum multiplexing," *Nat. Photonics* **6**(7), 488–496 (2012).
3. S. Li and J. Wang, "A compact trench-assisted multi-orbital-angular-momentum multi-ring fiber for ultrahigh-density space-division multiplexing (19 rings \times 22 modes)," *Sci. Rep.* **4**, 3853 (2014).
4. P. Gregg, P. Kristensen, and S. Ramachandran, "Conservation of orbital angular momentum in air-core optical fibers," *Optica* **2**(3), 267–270 (2015).
5. S. Ramachandran, P. Gregg, P. Kristensen, and S. E. Golowich, "On the scalability of ring fiber designs for OAM multiplexing," *Opt. Express* **23**(3), 3721–3730 (2015).
6. C. Brunet, P. Vaity, and L. A. Rusch, "Design, fabrication and validation of an OAM fiber supporting 36 modes," *Opt. Express* **22**(21), 26117–26127 (2014).
7. C. Brunet, B. Ung, L. Wang, Y. Messaddeq, S. LaRochelle, and L. A. Rusch, "Design of a family of ring-core fibers for OAM transmission studies," *Opt. Express* **23**(8), 10553–10563 (2015).
8. P. Gregg, P. Kristensen, S. Golowich, J. Olsen, P. Steinvurzel, and S. Ramachandran, "Stable transmission of 12 OAM states in air-core fiber," in *CLEO (OSA, 2013)*, paper CTu2K.2.
9. Y. Jung, E. L. Lim, Q. Kang, T. C. May-Smith, N. H. L. Wong, R. Standish, F. Poletti, J. K. Sahu, S. U. Alam, and D. J. Richardson, "Cladding pumped few-mode EDFA for mode division multiplexed transmission," *Opt. Express* **22**(23), 29008–29013 (2014).
10. G. Le Coq, Y. Quiquempois, A. Le Rouge, G. Bouwmans, H. El Hamzaoui, K. Delpace, M. Bouazaoui, and L. Bigot, "Few mode Er³⁺-doped fiber with micro-structured core for mode division multiplexing in the C-band," *Opt. Express* **21**(25), 31646–31659 (2013).
11. S. Ramachandran and P. Kristensen, "Optical vortices in fiber," *Nanophotonics* **2**(5–6), 455–474 (2013).
12. E. L. Lim, Q. Y. Kang, M. Gecevicius, F. Poletti, S. Alam, and D. J. Richardson, "Vector mode effects in few moded erbium doped fiber amplifiers," in *OFC (OSA, 2013)*, paper OTu3G.2.

13. Q. Y. Kang, P. Gregg, Y. Jung, E. L. Lim, S. Alam, S. Ramachandran, and D. J. Richardson, "Amplification of 12 OAM states in an air-core EDF," in *OFC (OSA, 2015)*, paper Tu3C.2.
14. K. S. Abedin, T. F. Taunay, M. Fishteyn, D. J. DiGiovanni, V. R. Supradeepa, J. M. Fini, M. F. Yan, B. Zhu, E. M. Monberg, and F. V. Dimarcello, "Cladding-pumped erbium-doped multicore fiber amplifier," *Opt. Express* **20**(18), 20191–20200 (2012).
15. K. S. Abedin, J. M. Fini, T. F. Thierry, B. Zhu, M. F. Yan, L. Bansal, F. V. Dimarcello, E. M. Monberg, and D. J. DiGiovanni, "Seven-core erbium-doped double-clad fiber amplifier pumped simultaneously by side-coupled multimode fiber," *Opt. Lett.* **39**(4), 993–996 (2014).
16. S. Jain, Y. Jung, T. C. May-Smith, S. U. Alam, J. K. Sahu, and D. J. Richardson, "Few-mode multi-element fiber amplifier for mode division multiplexing," *Opt. Express* **22**(23), 29031–29036 (2014).
17. A. Hardy and R. Oron, "Signal amplification in strongly pumped fiber amplifiers," *IEEE J. Quantum Electron.* **33**(3), 307–313 (1997).
18. W. H. Press, S. A. Teukolsky, W. T. Vetterling, and B. P. Flannery, *Numerical Recipes in C (2nd ed.): The Art of Scientific Computing* (Cambridge University Press, 1992).
19. S. Akhtari and P. M. Krummrich, "Impact of Mode Beating Effects between Pump Modes in Optical Multi Mode Amplifiers for Spatial Division Multiplexing," *IEEE Photonics Technol. Lett.* **25**(3), 4–6 (2013).

1. Introduction

It is well known that photons can carry orbital angular momentum (OAM), characterized by a helical phase front, $\exp(iL\varphi)$, where L can take any integer value, positive or negative, and it is referred to as the topological charge. Recently, the use of OAM modes as orthogonal signal channels in communication systems has gained much interest [1–6]. To date, two classes of fiber have supported OAM guidance. In the first class based on solid-core fiber designs (e.g. the vortex fiber [1] and the ring-core fiber [7]), MIMO-free transmission of low-order OAM modes over 1 km length of vortex fiber has been achieved [1]. However, solid-core fibers are typically incapable of transmitting higher-order OAM modes, because either the fiber's effective V-number is not sufficient, or the vector splitting of the higher-order OAM modes becomes small. The second class features an air core and an annular raised-index region that guides light [4,6,8]. The high index-contrast of the air-glass interface enables a large effective-index splitting among the vector (HE/EH) modes of the same $|L|$ family, which significantly reduces the modal crosstalk and allows stable transmission of OAM modes, even for high orders of $|L|$. Higher-order OAM modes have also been theoretically postulated to have better tolerance to fiber ellipticity and birefringence [3,4] and experimentally demonstrated to resist bend perturbations [4]. Hence, they seem suitable for long-distance transmission. In ref [4], stable propagation of high order OAM modes over 1km length has been experimentally demonstrated in an appropriately designed air-core fiber. The development of in-line OAM mode amplifiers is essential for the serious consideration of fiber communication network based on OAM modes. Similar to few-mode erbium-doped fiber amplifiers (FM-EDFAs) [9, 10] used in few-mode transmission, the differential modal gain (DMG) for independent OAM modes will be a key characteristic of OAM EDFAs and must be minimized to optimize the system performance.

In this work, we present modeling results on the amplification of 12 OAM modes (i.e. $|L| = 5, 6, 7$ for all combinations of L and S , with S representing spin) over the C-band in an air-core fiber (that matches with the state-of-the-art OAM passive fiber [4]) under either core- or cladding-pumping at 980 nm. Under the core pumping condition with a uniform erbium ring doping profile, we found that pumping using the OAM modes of $|L| = 8$ provides the lowest DMG of 0.25 dB at 1550 nm among the signal modes of $|L| = 5, 6$ and 7, whilst most other choices of pump modes would create a DMG > 1 dB. Next, we explored the use of a radially confined erbium dopant profile, (in addition to the choice of pump mode group), to provide an additional degree of design freedom to help minimize DMG. Our results show that a confined doping profile doesn't necessarily remove the DMG dependency on pump modes, but it can help to increase the number of desired pump modes that provide a low DMG. Finally, we consider the more desirable/practical case of cladding-pumped operation where the pump mode dependency is almost removed. We find that there is a ~ 2.5 dB gain difference between the signal modes when the annular ring core is uniformly doped with erbium. However, with

an optimized erbium-doping profile, we achieve exceptionally well equalized modal gain (DMG ≤ 0.25 dB) for all 12 OAM modes.

2. Modeling of the amplification of OAM modes in air-core fiber

Figure 1(a) shows the refractive index profile (RIP) of the proposed air-core EDF, which matches with the state-of-the-art passive air-core OAM fiber demonstrated in ref [4]. The inner radius (r_1) of the air core is 3 μm , the outer radius (r_2) is 8.25 μm , and the refractive index difference between the annular guiding region and the silica cladding is 0.035. The rationale of the air-core fiber design can be found in ref [4]. The air-core fiber guides up to the $|L| = 7$ OAM family in C-band wavelengths (1530-1565 nm). Here, the OAM modes are identified as $\text{OAM}_{(L,m)}$, where L is the topological charge, and m is the number of concentric rings in the intensity profile of the mode [6, 11]. The modal intensity profiles of $\text{OAM}_{(L,1)}$ $|L| = 5, 6$ and 7 modes are shown in Fig. 1(a). Figure 1(b) shows the effective index difference between the vector modes (i.e. HE/EH modes) from the same $|L|$ family ($m = 1$) as a function of wavelength. Figure 1(b) shows that a large effective index splitting is observed among the high-order OAM families (i.e. $|L| = 5, 6$ and 7), which makes these OAM modes more resilient to perturbations as they propagate along the fiber. The low-order $\text{OAM}_{(L,1)}$ modes ($|L| = 1-4$) are not considered in this work due to the insufficient vector splitting which would make these modes prone to mode coupling. The double ring modes (i.e. $\text{OAM}_{(0,2)}$ - $\text{OAM}_{(3,2)}$) are also guided in the air-core fiber at 1550 nm, but again these modes are not considered in this work for two reasons. Firstly, if the double ring modes become degenerate in some wavelength regime with the high-order ring modes, phase-matched cross-coupling is possible. Secondly, passive fiber coupling and transmission of such states have not yet been demonstrated.

The core-pumped OAM mode amplifier was simulated using the vector-mode FM-EDFA simulator described previously [12, 13], for which $\text{OAM}_{(L,m)}$ modes are described as: $\text{OAM}_{\pm L,m}^{\pm} = \text{HE}_{L+1,m}^{\text{even}}$ and $\text{OAM}_{\mp L,m}^{\mp} = \text{EH}_{L-1,m}^{\text{even}} \pm i\text{EH}_{L-1,m}^{\text{odd}}$ [11], where the superscript denotes spin, or the handedness of circular polarization. The vector fields of the signal and pump modes are computed using COMSOL Multiphysics® software. For all the simulations in this work, we model the simpler case of a co-propagating pump, to speed up simulations and facilitate the exploration of a wider range of pump modes and design parameters.

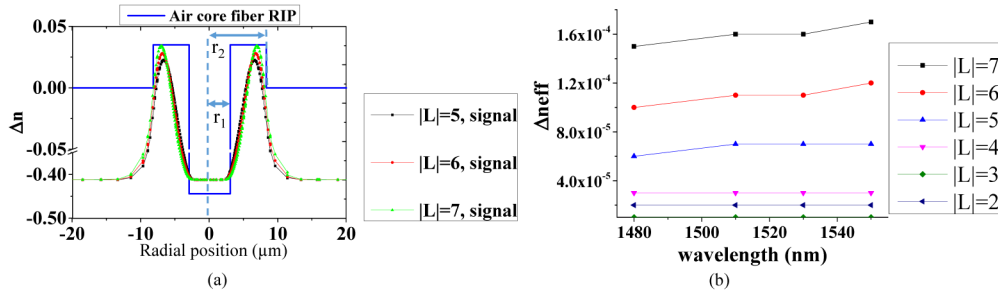


Fig. 1. (a) The RIP of the air-core fiber overlaid with the normalized signal intensity profile of the OAM states $|L| = 5, 6, 7$. (b) the effective index difference (Δn_{eff}) between the vector modes within the same $|L|$ family as a function of wavelength, for radial order $m = 1$.

3. Results and discussions

3.1 Core-pumped operation

At 980 nm, this fiber guides 110 vector modes (i.e. including degeneracies), which can be grouped into 29 (L, m) OAM families and $\text{TM}_{0,m}$, $\text{TE}_{0,m}$ (i.e. $m = 1, 2, 3$) modes. Each $\text{OAM}_{(|L|, m)}$ ($|L| = 0, 1$) family has two OAM modes, while each $\text{OAM}_{(|L|, m)}$ ($|L| \neq 0, 1$) family has four OAM modes. In order to completely describe how each pump mode impacts the

DMG among the $|L| = 5, 6,$ and 7 signal modes, we assessed the 110 pump modes individually. In each simulation run, only one pump mode was launched into the OAM amplifier. The pump power was set to 200 mW and the input signal (at 1550 nm) power was set to -20 dBm per OAM mode. We chose the amplifier length (i.e. around 5 m with small variations depending on the pump mode) at which the amplified total signal power reaches its maximum. The erbium doping profile is assumed to be uniform within the annular guiding region with a doping concentration of $1.5 \times 10^{25} \text{ m}^{-3}$. Due to the circular symmetry of the air-core fiber, the simulated DMGs denoted by ΔG in Fig. 2 using different pump modes that belong to the same $\text{OAM}_{(L,m)}$ family (e.g. the $\text{OAM}_{2,1}^+$ and $\text{OAM}_{-2,1}^+$ modes of the $\text{OAM}_{(2,1)}$ family) are nearly identical. The calculated DMGs using the $\text{TM}_{(0,m)}$ and $\text{TE}_{(0,m)}$ modes resemble those using $\text{OAM}_{(1,m)}$ families, due to similar modal intensity profiles. Similarly, the gains for different signal modes that belong to the same OAM family (e.g. $\text{OAM}_{5,1}^+$ and $\text{OAM}_{-5,1}^+$) are nearly identical. We summarize the 29 possible pump OAM families and their corresponding DMGs into three groups, according to their radial mode orders (i.e. $m = 1, 2, 3$), as shown in Fig. 2. The physical origin of the DMG results from differences in the overlap of the pump modes, signal modes and the distribution of the rare-earth dopant. The observed variation of DMGs for different pump modes is expected, as the pump mode intensity varies according to the mode order. As shown by the pink highlighted region in Fig. 2, the best pump family that provides the lowest DMGs (i.e. ~ 0.25 dB) is $\text{OAM}_{(8,1)}$. In comparison, the calculated DMG is about 3.1 dB when pumped by $\text{OAM}_{(0,1)}$, because the $\text{OAM}_{(0,1)}$ pump has a much better overlap with the $\text{OAM}_{(5,1)}$ signal mode over the $\text{OAM}_{(7,1)}$ signal mode. Finally, we present the modal gain spectrum using WDM signals pumped by the $\text{OAM}_{(8,1)}$ mode as shown in Fig. 3. Eight wavelength channels spaced equally from 1530 nm to 1565 nm, and 12 OAM modes at each wavelength with the power of -20 dBm per mode per wavelength were used as the input signals. As the total input signal power increased 8-fold compared with the simulations performed at single signal wavelength, the pump power was set to be 450 mW in order to maintain the modal gains above 20 dB. The fiber length was chosen to be 3.5 m in order to balance the gain between short (i.e. 1530 nm to 1535 nm) and long (i.e. 1550 nm to 1565 nm) wavelengths. As shown in Fig. 3, the DMGs across the whole C band are found to be below 1 dB, with the highest of 1 dB at 1530nm and the lowest of 0.2 dB at 1550nm.

Although very low DMG can theoretically be achieved with the $\text{OAM}_{(8,1)}$ mode, in practice the excitation of a pure $\text{OAM}_{(8,1)}$ pump may be challenging. It is also possible that significant power will couple into other pump modes (for example, $\text{OAM}_{(8,2)}$) and compromise amplifier performance. In addition, the insertion loss can potentially be quite high to excite high-order pump modes, such as $\text{OAM}_{(8,1)}$ from a single-mode pump diode without the use of high precision or custom components, which makes the OAM EDFA very expensive and less practical.

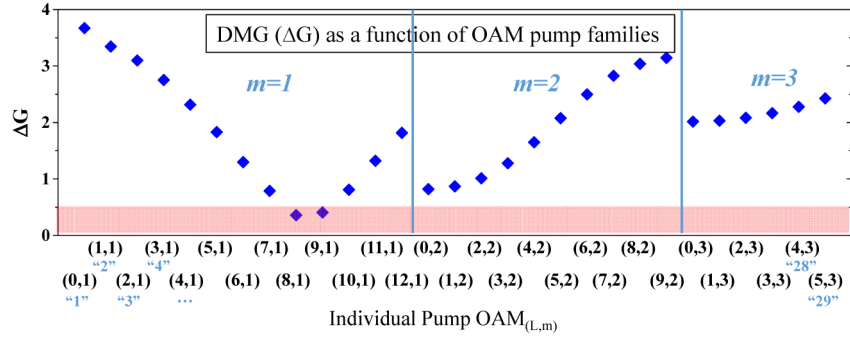


Fig. 2. The distribution of DMGs and their corresponding pump $OAM_{(L,m)}$, plotted in order of decreasing mode effective index that of the same “m” group. The blue numbers (e.g. “1”, “2”) under the mode labels corresponds to the mode number shown in Fig. 4(b).

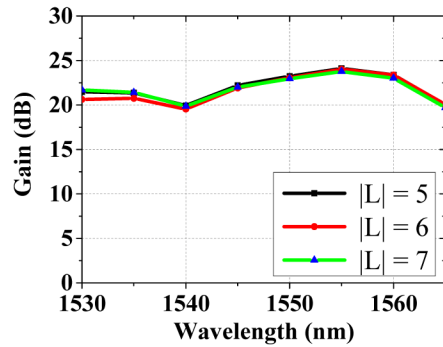


Fig. 3. The gain profile of WDM OAM signals with the $OAM_{(8,1)}$ pump mode.

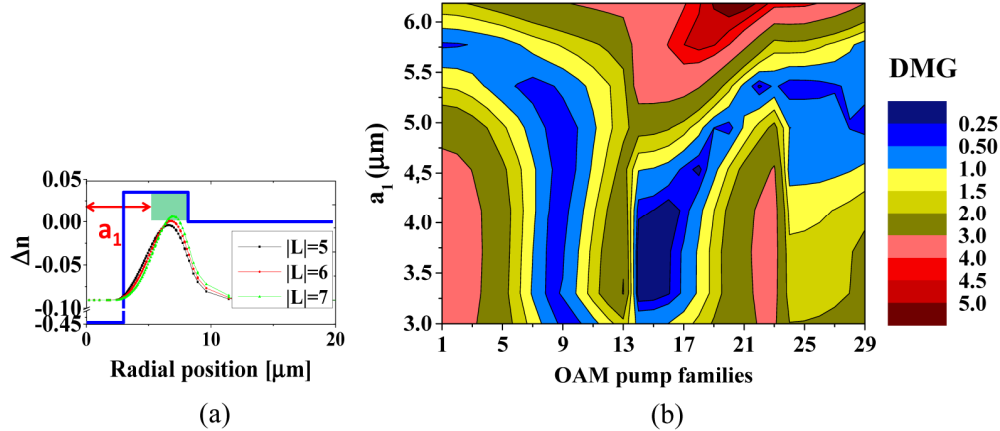


Fig. 4. (a) The confined doping structure determined by parameter a_1 in the air core OAM amplifier. (b) The contour plots of the DMGs (ΔG) against the 29 pump $OAM_{(L,m)}$ families (correspond to the pump modes listed in Fig. 2) and the variation of a_1 .

In the following discussion, we investigate whether using a confined doping profile can reduce the strong modal gain dependence on pump families observed in the fully doped case discussed above. The parameter a_1 is introduced to determine the dimension of the confined doping distribution inside the annular guiding region, as shown in the insert of Fig. 4(a). The contour plots shown in Fig. 4(b) summaries the DMG (ΔG) as a function of the OAM pump families and the variation of a_1 . The same input signal and pump power levels are used for

Fig. 4(b) as in Fig. 2. The fiber length was set to 5 m. a_l was tuned from 3 μm (i.e. the fully doped case) to 6.2 μm (i.e. for $a_l > 6.2 \mu\text{m}$, the overlap between the erbium and the signals reduces significantly). As shown in Fig. 4(b), generally the DMGs still exhibit a strong dependence on the OAM pump families when the confined doping profiles are considered. As different pump modes overlap differently with the erbium ions, in this OAM EDFA a certain doping profile would only favour specific pump modes to ensure low ΔG among the 12 OAM signal modes. However, using this approach of tuning a_l , we find that in the region of $a_l = 5.1$ to 5.3 μm , $\Delta G < 1$ dB (corresponds to the blue region in Fig. 4(b)) can be achieved using any pump modes ranging from (1) $\text{OAM}_{(7,1)}$ to $\text{OAM}_{(11,1)}$ from the $m = 1$ group, (2) $\text{OAM}_{(5,2)}$ to $\text{OAM}_{(7,2)}$ from the $m = 2$ group, (3) all the modes from the $m = 3$ group. Consequently, tailoring the erbium doping profile (i.e. confined doping) is likely give a larger tolerance on the pump mode excitation for this core-pumped OAM EDFA to deliver high gain and low ΔG . Alternatively, to remove the concern of the pump mode dependency, one can consider the case of cladding pumping.

3.2 Cladding pumped operation

Cladding pumping has the advantages of very high pump-powers (i.e. $>10\text{W}$) available from multimode pump diodes and a much lower cost compared with the single-mode pump diode in term of $\$/\text{W}$ [9]. The cladding pumping scheme had already been experimentally demonstrated as an efficient and practical way to provide pump sharing for multiple spatial channels in multi-core EDFAs [14, 15], 6-spatial-mode EDFA [9] and few-mode multi-element EDFAs [16]. The pump light can be side coupled into the double-clad active fiber using a tapered multimode pump fiber [15]. In the modeling of cladding-pumped amplifiers, a simple but effective way to simulate the pump is to assume that the pump intensity profile is uniform across the doped core [17]. Consequently, in the amplifier design region, the erbium doping profile is the only degree of freedom that we can tailor to minimize ΔG , here, controlled by the value of a_l . The inner cladding is assumed to be 70 μm in diameter and the pump power is set to 2.5 W, which creates a uniform pump intensity of $6.5 \times 10^8 \text{ W/m}^2$ at the input end of the fiber. The input signal at 1550 nm power is set to -10 dBm per OAM mode. We chose the amplifier length at which the amplified total signal power reaches its maximum, around 4 m in this instance. For the simulations shown in Fig. 5(a), the noise calculation was ignored to facilitate fast computation and explore the optimal doping profile for cladding pumped operation. As shown in Fig. 5(a), the DMG reduces as a_l increases from 3 μm to 5.2 μm , and increases again when a_l becomes larger than 5.2 μm . When the annular guiding region is fully doped, the $|L| = 5$ group has a larger gain than that of the $|L| = 7$ group due to the better overlap with the gain medium, and a DMG of 2.5 dB is observed. Conversely, when the doped region becomes slim (i.e. $a_l > 5.2 \mu\text{m}$), the $|L| = 7$ group sees the advantage of being amplified more than the $|L| = 5$ group. The optimal design is given by $a_l = 5.2 \mu\text{m}$, where the gain for the three OAM signal groups are balanced and the minimal ΔG is found to be 0.25 dB.

Finally, the WDM gain profiles of the cladding-pumped OAM amplifier using the optimal value of a_l was examined. Eight wavelength channels spaced equally from 1530 nm to 1565 nm, and 12 OAM modes at each wavelength with the power of -20 dBm per mode per wavelength were used as the input signals. The fiber length was chosen empirically to be 4 m in order to balance the gain between short (i.e. 1530 nm to 1535 nm) and long (i.e. 1550 nm to 1565 nm) wavelengths. In order to evaluate the noise figure (NF) of the cladding pumped OAM EDFA, the amplified spontaneous emission (ASE) added by the amplifier must be calculated. The noise wavelengths were set to be identical to those of the WDM signals, thus giving a noise bandwidth of 5 nm each. The WDM gain profiles and the NF for OAM modes with $|L| = 5, 6,$ and 7 are shown in Fig. 5(b). Since the OAM EDFA guides OAM modes (i.e. and also $\text{TE}_{0m}, \text{TM}_{0m}$ modes) up to the order of $|L| = 7$ in the 1.5 μm wavelength range, ASE will be generated among all these guided modes. With so many ASE components to handle

simultaneously, a “relaxation method” [18] was applied to numerically solve the heavily multimode ASE. The vanishingly small ASE both at $L = 0\text{m}$ and $L = 4\text{m}$ shown in Fig. 6(a) is a clear evidence that the numerical model has converged and that the ASE profiles we obtained are reasonably correct. Fig. 6(b) presents the normalized population inversion along the fiber length, which shows that the backward ASE plays significant role in suppressing the population inversion (i.e. N_2) at the beginning of the OAM EDFA compromising the modal gains. Although the full vector treatment was applied in the simulation, the modal beating effect [12,] [19] is not significantly pronounced in the inversion profiles along the fiber length (i.e. see Fig. 6(b)). This is because firstly the beating length of the positive L OAM and negative L OAM modes of the same spin are very small (in the region of “mm”), so the beating effect is averaged out over meter length scales. Secondly, the beating effect among the high-order OAM modes (i.e. $|L| = 5, 6, 7$) does not create a significant difference on the overall overlap between the signal intensity and erbium ions compared with the case of the LP_{11} signal mode discussed in [12]. It can be seen that the gain curves for different spatial modes overlap with each other at all wavelengths within the C-band to within 0.25 dB, thus providing excellent modal gain performance. The NFs are found to be between 4 dB to 5.2 dB, which are in the typical range of cladding-pumped EDFAs.

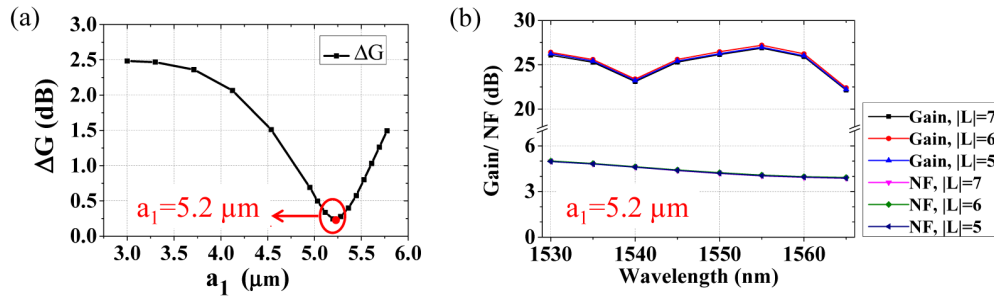


Fig. 5. (a) DMG as a function of a_1 for cladding pumping operation. (b) The gain and NF of the WDM OAM signals with $a_1 = 5.2 \mu\text{m}$.

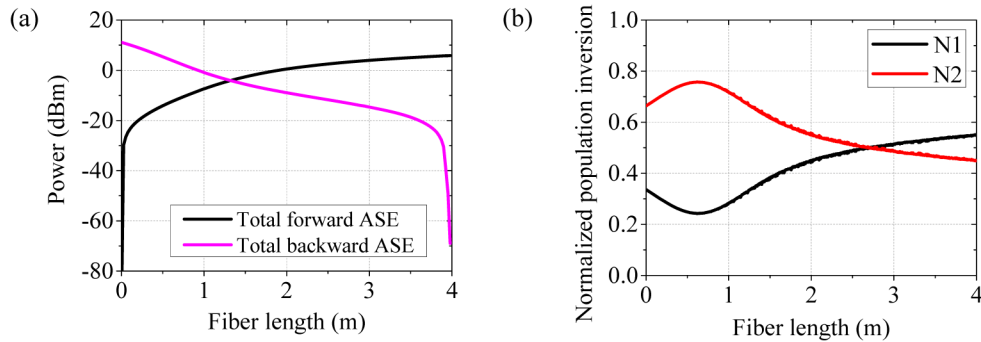


Fig. 6. The cladding-pumped OAM EDFA with $a_1 = 5.2 \mu\text{m}$: (a) Evolution of the total power of the forward and backward ASE along the fiber length. (b) The normalized population inversion along the fiber length.

4. Conclusions

We modeled the amplification of 12 OAM modes (i.e. $|L| = 5, 6$ and 7) in an air-core EDF over the C-band. Under the core pumping condition based on a fully doped core, we assessed the performance of all the supported pump modes (i.e. 110 in total) individually, and observed that the $OAM_{(8,1)}$ pump mode provided the lowest DMG of 0.25 dB at 1550nm, whilst most of the other pump modes resulted in $DMG > 1$ dB. The DMG dependence on pump modes is

also strong for confined doping profiles. However, through tailoring the erbium doping profile, we can increase the number of suitable pump modes which deliver $\Delta G < 1$ dB for the core-pumped OAM amplifier. Alternatively, a more cost effective way to provide pump radiation is cladding pumping. In addition, it can remove the concern of pump mode dependency. Using an optimized double-clad EDF design, DMGs of 0.25 dB and small signal gain of more than 20 dB can be achieved for the 12 OAM modes across the full C-band.

Acknowledgments

This work is supported in part by the UK EPSRC grant EP/J008591/1 (COMIMO), the DARPA InPho program under grant nos. W911NF-12-1-0323 and W911NF-13-1-0103, and NSF grant no. ECCS-1310493. P. Gregg acknowledges support from NSF-GRP grant no. DGE-1247312. Data associated with this publication can be accessed via URL <http://dx.doi.org/10.5258/SOTON/382894>.